

Negative Index of Reflection in Planar Metamaterial Composed of Single Split-Ring Resonators

Ming-Chun Tang, Shaoqiu Xiao, Duo Wang, Jiang Xiong, Kun Chen, and Bingzhong Wang

The Institute of Applied Physics

University of Electronic Science and Technology of China, Chengdu, China, 610054

xiaoshaoqiu@uestc.edu.cn

Abstract - This paper reports the negative index of refraction in planar metamaterial consisted of only a traditional single split-ring resonator (SRR), which is proved to exhibit simultaneously negative permittivity and negative permeability without the use of assistant metallic structures by retrieving the effective electromagnetic parameters. With the aid of current distributions investigation, it is demonstrated that within the left-handed band the negative permittivity is generated in a way analogous to the case of dual parallel cut-wire metamaterial, and negative permeability arises from the asymmetric second-order magnetic resonant mode.

Index Terms - Negative index reflection, negative permeability, negative permittivity, planar metamaterial, single SRR.

I. Introduction

In 2001, the fantastic negative refraction was accomplished by a prism made of left-handed material (LHM) [1, 2], which had been previously predicated by Veselago [3]. Since then, various kinds of LHMs have been constructed, such as SRR-shaped [4], Ω -shaped [5], brick-wall-shaped [6], cut-wire-shaped [7], S-shaped [8, 9], right-angle-shaped [10], H-shaped [11], chirality-shaped [12] resonators, and so on. Typically, these LHMs designs can be classified into two categories: one, like those reported in [1 and 4], is realized from separate arrays of periodically arranged split ring resonators that exhibit negative permeability and metallic wires that exhibit negative permittivity; the other, as proposed in [5–12], only uses sub-wavelength structures which incorporate traditional wires and SRRs into different combined patterns with simultaneous electric and magnetic resonances. However, most of these LHMs share

certain defects. For example, most metallic patterns are printed on both sides of the substrates [1, 5-8], and some lumped active elements (such as varactor diodes) are added in the design [8, 9], both of which increase the complexity of design and application; some LHMs resort to composite metamaterial units [10] or bear too long unit length along the electric polarized direction [11, 12], whose unit cell takes up too much space accordingly.

Given that their performances are qualitatively similar to those of double split-ring resonators (SRRs) [13], single SRRs have been utilized to design different kinds of metallic metamaterials, recently. As their electric resonance properties are just like cut wires, they have already seen applications in fabricating planar electric metamaterials [14-16]. On the other hand, being able to generate circulating currents, they have also been used to realize magnetic resonances [17-22]. Generally, a LHM could only function on the condition that the negative electric and magnetic responses are modulated to a common frequency band [1, 3]. However, since an ordinary single SRR has a much lower fundamental magnetic resonance frequency than that of the electric resonance, it is impossible to achieve a common frequency band after modulation. Therefore, no LHM composed of single SRR units have been reported yet.

In this paper, after a thorough numerical investigation of the resonance characteristics of a single SRR, we propose one new method to design LHM with a single SRR unit. In the design, we utilize the magnetic resonant frequency in asymmetrical second-order mode, and the electric resonant frequency in fundamental electric resonant mode. The two frequency bands, after subtle adjustment of unit dimension, are accommodated to

overlap very well; thus, contributing to the accomplishment of our expected LHM. It is of interest that, without resorting to additional lumped active elements or metallic cut wires, the proposed LHM unit is easily achieved and boasts a simple and uniform configuration.

II. NUMERICAL INVESTIGATION ON AN ORDINARY SINGLE SRR

The unit cell of an ordinary metallic single SRR metamaterial is schematically shown in Fig. 1. The single split ring with a thickness of 0.0017 mm is placed in the center of the cube with the dimensions $L_x \times L_y \times L_z = 15\text{mm} \times 15\text{mm} \times 15\text{mm}$, and the cube is filled with Rogers RT/duroid 5880 with relative dielectric constant $\epsilon_r = 2.2$. The detailed geometry of SRR is: the gap of ring $g = 1\text{mm}$, the outer radius $R = 6\text{mm}$, and the width $w = 1.1\text{mm}$.

The numerical simulations are all performed using the finite-element method (Ansoft's HFSS), whose accuracy has been already confirmed by its good agreement with experimental results as in literatures [23, 24]. A theoretical model based on an artificial waveguide with the transverse boundaries of two ideal magnetic conductors and two ideal electric conductor planes is employed. This enables the model to be equivalent to an infinite layer medium illuminated by a normal incident plane wave [25-27]. To be specific, input/output ports are imposed in x -direction, and perfectly electric conducting (PEC) and perfectly magnetic conducting (PMC) boundary conditions are imposed in y - and z - directions, respectively. It is noted that, the electric component of the electromagnetic wave perpendicular to the split bearing side of the ring (along y -axis) is adopted for the sake of eliminating the undesired bi-anisotropic effect via asymmetry [27, 28].

At first, we discuss the condition in Fig. 2. As sketched, the single SRR is placed where the electromagnetic wave propagates (in the x -direction) perpendicular to the SRR face (in the yz -plane) and external polarized magnetic field (in the z -direction) is parallel to its face. Shown in the simulated transmission spectrum, the SRR can be electrically excited around 7.35GHz (i.e., in the fundamental electric resonant mode), in agreement with the theoretical analysis in literature [29]. Further, the induced current distribution at 7.35GHz is presented. Obviously, the charge accumulates symmetrically on opposite arms of the ring, and the ring is in analogy

to the dual parallel connected cut-wires of the same dimensions. Thus, the ring can be viewed as two parallel LC resonant circuits operating in the fundamental modes. Owing to the same dimensions of the two arms, the two LC resonances are both operating in the same fundamental electric resonant frequency band.

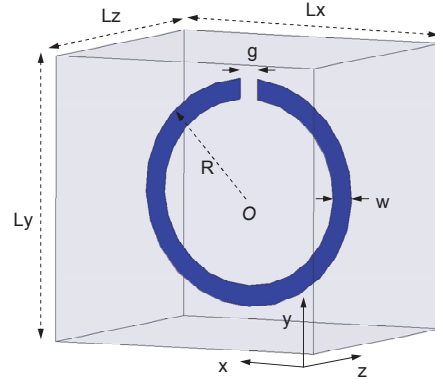


Fig. 1. The unit cell of the metallic metamaterial designed with single SRR.

Then, we rotate the SRR around y - axis for 90° in xz plane, shown in Fig. 3. In this simulation, the single SRR is placed where the electromagnetic wave propagates (in the x -direction) parallel to the SRR face (in the xy -plane). An external polarized magnetic field (in the z -direction) is perpendicular to its face, which can induce magnetic response in addition to electric response. The corresponding simulated transmission spectrum is, also, presented in Fig. 3. There are three dips appearing within this frequency region. As is aforementioned, the third dip at 7.35GHz results from the external electric excitation. Therefore, the other two dips (including 2.7GHz and 6.35GHz) could only be caused by external magnetic excitation, since the bi-anisotropic effect has been eliminated [28].

In order to confirm its resonance mechanism, the current distributions at each dip are demonstrated in Fig. 4. It is obvious that the circling current is induced by the external magnetic field, which incurs a magnetic response in fundamental mode around 2.7GHz in Fig. 4(a) [22]. Naturally, the corresponding second-order mode (i.e., the dip at 6.35GHz in Fig. 3) could occur at a higher resonant frequency. For clarity, the current distributions at the higher mode are demonstrated in Fig. 4(b). It is noted that, the current distribution in second-mode is

non-uniform and asymmetric [30]. This can be ascribed to the following two main reasons; one is that there is no intrinsic symmetric even-mode current distributions existing based on magnetic excitation in this type of SRR. As is well known, the polarization currents are directly contributed by external magnetic field [13, 31], whenever the SRR is excited at the arbitrary-order magnetic resonant modes. It can be assumed that, if the magnetic resonances in even-modes were symmetric, the current distributions should also be symmetrically distributed at the two arms (just like aforementioned electric resonance in fundamental mode in Fig. 2). Eventually, it would lead the sum of the even-mode response for the external magnetic field to be zero, i.e., the external magnetic field would make no contribution to the overall SRR magnetic response. The other reason is that, the other kind of response (electric response in the fundamental mode at 7.35GHz) is quite near to the magnetic response in the second-mode 6.35GHz in Fig. 3, and those nearby responses could exhibit mutual coupling between each other, which disturbs current distributions. For the electric resonance in the fundamental mode, because of the influence of nearby magnetic excitation, the current distributions induced by the external electric field in the two paralleled arms depicted in Fig.4(c) are apparently not as symmetric as in Fig. 2

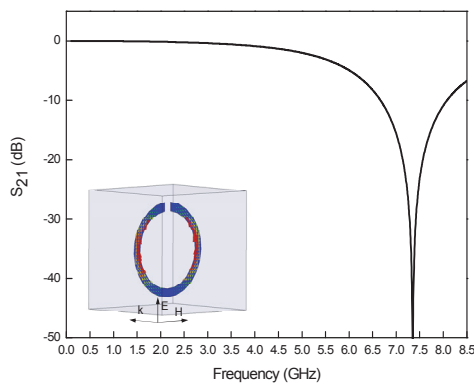


Fig. 2. The simulated transmission spectrum and current distribution (at the dip 7.35GHz), when the single SRR is only electric excited.

III. NEGATIVE INDEX OF REFRACTION ENABLED BY SINGLE SRRS

As is known, negative permittivity can be achieved by the electric resonance, and negative permeability can be ensured by magnetic resonance analogously. It is aforementioned in Section II that the ordinary single SRR would usually exhibit electric resonance and magnetic resonance at different frequencies, as shown in Fig. 3. However, negative refraction requires a negative permittivity and a negative permeability at a common frequency range, which necessitates certain overlapping frequency range of the electric resonance and magnetic resonance frequency of single SRR.

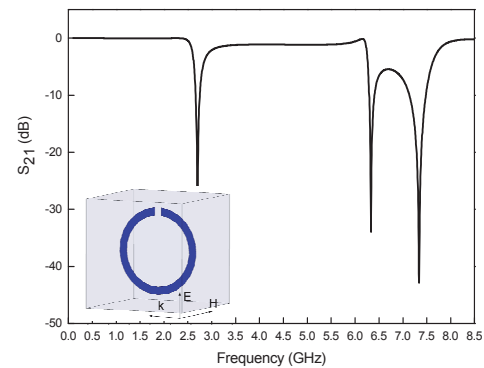


Fig. 3. The simulated transmission spectrum on the condition that the single SRR is both electrically and magnetically excited.

Considering the electric resonant frequency in fundamental mode is near to the magnetic resonant frequency in second-order mode, a parametric study is carried out in order to make the two resonance frequency bands closer by adjusting the SRR dimensions as shown in Fig. 5. Firstly, the effect of the split gap (g) is numerically studied. From Fig. 5(a), it is observed that the split gap has little impact on the distance between the two resonance frequency bands. When the split gap becomes

larger, the electric resonance frequency goes up in accordance with the two magnetic resonance frequencies. The main reason is that the enlargement of split gap results in the reduction of the effective electric length along the E-polarized direction induced by an external electric field, and the decrease of the effective circulating current path and split capacitance induced by an external magnetic field. This leads to the increase of electric resonance frequency (ω_{eo}) and each magnetic resonance frequency (ω_{mo}). The effect of the SRR width (w) has also been studied in Fig. 5(b). As mentioned above, the single SRR is in analogy to the dual

when w goes narrower, the above two resonant frequencies get closer. Especially, the two resonant frequency regions occupy overlapping band (in the dotted zone) when $w=0.2\text{mm}$, leading to a narrow passband centered at 6.4GHz occurrence. Thirdly, the effect of the radius (R) of metallic SRR on the resonance frequency has been investigated shown in Fig. 5(c). When the radius (R) goes up, both of the ω_{eo} and ω_{mo} are simultaneously dropping. We ascribe this phenomenon to that, the increase of R brings about the corresponding enlargement of the effective electric length along the E-polarized direction induced by an external electric field, and also the increase of the effective circulating current path induced by an external magnetic field, simultaneously.

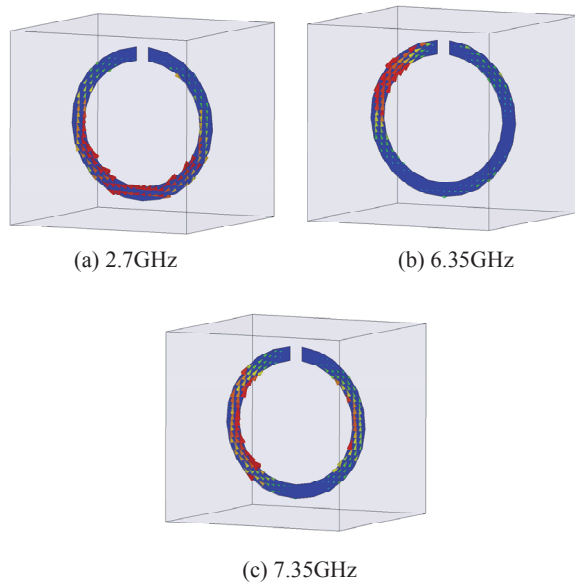
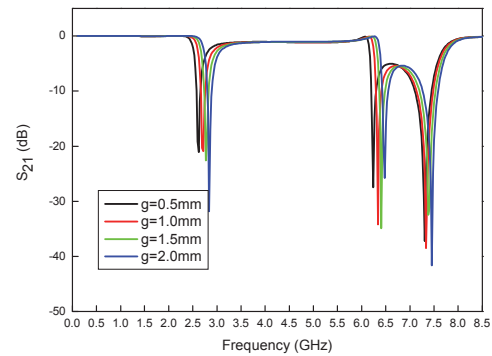
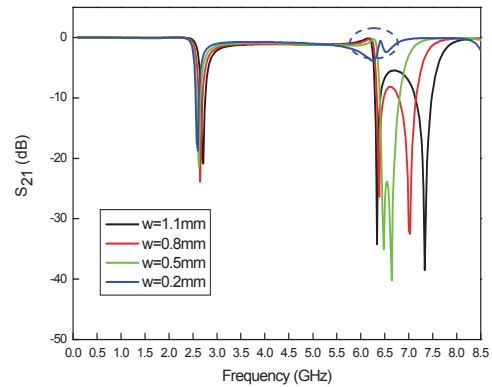


Fig. 4. Current distributions at three different resonant dips. (a) The fundamental magnetic resonant frequency; (b) The second-order magnetic resonant frequency; (c) The fundamental electric resonant frequency.

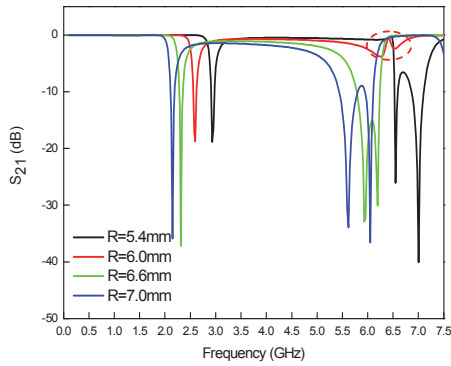
parallel connected cut wires. Hence, by decreasing the width of SRR (which is equivalent to the effective radius of cut wire in literature [32]), the corresponding ω_{eo} drops distinctly. Meanwhile, its influence on the ω_{mo} can be neglected except a little variation due to the small difference in split capacitance. Therefore, in Fig. 5(b) it is of our interest that,



(a)



(b)

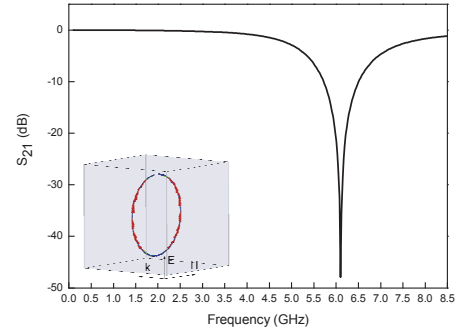


(c)

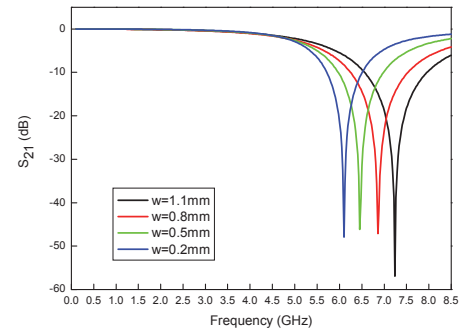
Fig. 5. The effect of metallic SRR dimensions on the resonance frequency; (a) the split gap (g), (b) the width (w), the radius (R).

Furthermore, in order to judge the existence of the electric resonance around 6.4GHz in Fig. 5 easily, we also rotate the SRR around y -axis for 90° in xz plane, with the electromagnetic environment the same as Fig. 2. Fig. 6(a) demonstrates that the SRR provides a stopband near 6.1GHz, exhibiting strong electric response (according to the current distribution on the two arms at the dip 6.1GHz) in analogy with the simulated result in Fig. 2. It verifies that there is also a strong electric resonance occurring within the passband. Logically, the magnetic resonance also exists in the passband to ensure negative index of refraction. Moreover, Fig. 6(b) shows the effect of SRR width (w) on the resonance frequency, when the single SRR is only electric excited (i.e., it is placed in the same electromagnetic environment as that in Fig. 6(a)). Apparently, when the W goes narrower, the electric resonance frequency (ω_{eo}) drops distinctly (from 7.24GHz to 7.10GHz), which is in good accordance with the results in Fig. 5(b), thus confirming the validation of our aforementioned theory [32].

To further confirm the effectiveness of our proposed LHM design, a retrieval calculation is performed to obtain the effective permittivity ϵ_{eff} and the effective permeability μ_{eff} from the scattering parameters S_{21} and S_{11} of the proposed SRR metamaterial. According to literature [33],



(a)



(b)

Fig. 6. The simulated transmission spectrum when the single SRR is only electric excited; (a) the transmission spectrum and the current distribution (at the dip 6.1GHz), (b) the effect of SRR width (w) on the resonance frequency.

in order to attain electromagnetic parameters (including permittivity and permeability), the refractive index (n) and the wave impedance (z) is firstly obtained from Equations (1) and (2), respectively, and then the electromagnetic parameters are acquired from Equations (3) and (4), respectively.

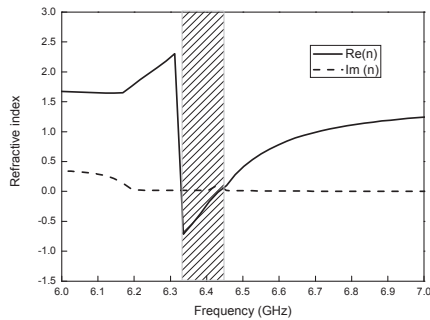
$$n = \frac{1}{kd} \cos^{-1} \left[\frac{1}{2S_{21}} (1 - S_{11}^2 + S_{21}^2) \right]. \quad (1)$$

$$z = \sqrt{\frac{(1 + S_{11})^2 - S_{21}^2}{(1 - S_{11})^2 - S_{21}^2}}. \quad (2)$$

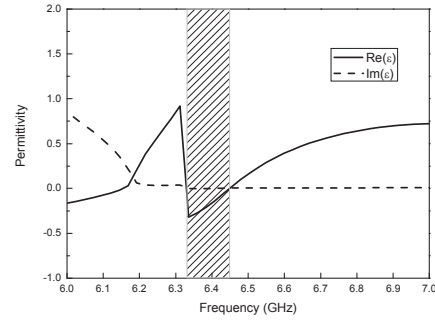
$$\varepsilon = \frac{n}{z}. \quad (3)$$

$$\mu = nz. \quad (4)$$

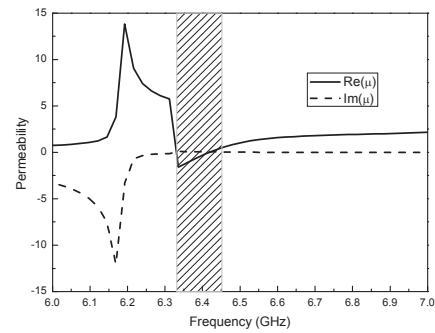
It is noted, in the retrieval procedure the Kramers–Kronig relations is applied to achieve the uniqueness of their values here [34]. The retrieved results in Fig. 7 demonstrate that, within the negative refractive index frequency band, the ε_{eff} and μ_{eff} are simultaneously negative corresponding to the passband region from 6.34GHz to 6.45GHz, which is also the overlapping region between fundamental electric resonant frequency band and second-order magnetic resonant frequency band. Thus, the retrieved datas are consistent with the results concluded earlier. Also, Fig. 7 shows the imaginary parts of permittivity and permeability are relative smooth and almost zero, which indicate very weak anti-resonances and low losses of our proposed LHM unit in spite of its very simple configuration [35]. However, it is also worth mentioning that, our proposed LHM can only provide a much narrower bandwidth (with only 3.4% fractional bandwidth) with negative index of reflection than LHM proposed in literature [33].



(a)



(b)



(c)

Fig. 7. Retrieved electromagnetism parameters of the metamaterial composed of SRRs from the scattering parameters in Fig. 5 where both electric and magnetic excitations provided ($w=0.2\text{mm}$); (a) refractive index, (b) permittivity, and (c) permeability.

In addition, the current distributions under different excitations at different phases have been compared and discussed in Fig. 8. Figs. 8(a) and (b) present the current distributions, when the SRR is excited by time-varying external electric field and magnetic field, respectively [31]. As is well known that, the different resonances come from in phase and out of phase responses of the structure with the driving incident field, due to the different excitations. It is further attested in Fig. 8(a) that the relatively symmetric charge distribution at both arms of SRR is observed when there is only electric excitation, while the majority of charges are accumulated at only one arm when only magnetic excitation provided in Fig. 8 (b). And

it deserves to be mentioned that, the electric response is more significant at phases 90° , and 135° , while magnetic response is more significant at phase 45° . In Fig. 8 (c), the majority of charges accumulate at two arms in approximately symmetrical distribution at phase 135° , just like that in Fig. 8 (b). Meanwhile, the majority of charges accumulate at only one arm at phase 45° also like that in Fig. 8 (a), exhibiting distinctly asymmetric current distributions. This phenomenon that there is also most of the asymmetric current distributions on the two legs at 90° in Fig. 8 (c), can be ascribed to the strong mutual coupling between the magnetic and electric responses centered at the nearby phases (shown in Fig. 8 (a) and 8 (b), respectively). The above phenomenon further validates the existence of the simultaneously electric and magnetic responses, and confirms the accomplishment of the LHM design.

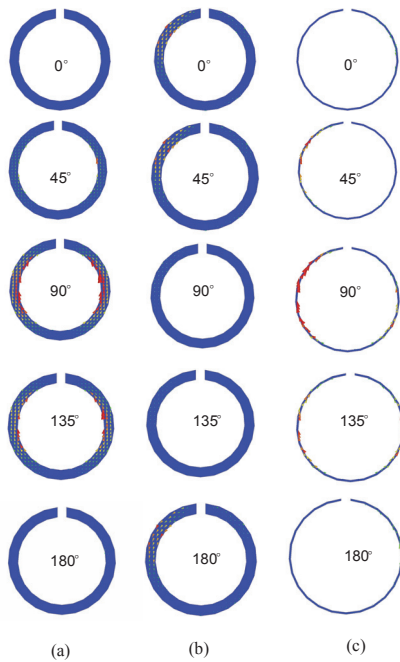


Fig. 8. Current distributions at different phases within half of a period. (a) Only electric excitation at the dip 7.35GHz in Fig. 2; (b) second-order magnetic excitation at the dip 6.35GHz in Fig. 4(b); (c) both electric and magnetic excitations at 6.53GHz for proposed LHM unit.

IV. CONCLUSION

We have numerically investigated the left-handed response in metallic metamaterial comprised of single SRRs. It is learned from simulation data that the electric response in the fundamental mode and magnetic response in second-mode for the traditional single SRR is very near. By adjusting the geometric parameters of the SRR configuration, a simple LHM without using additional metallic wires can be easily realized.

ACKNOWLEDGEMENT

The authors would like to express their thanks to the anonymous reviewers for their careful reading of the manuscript, and their constructive suggestions for the improvement of our work. And the work was in part supported by the National Nature Science Foundation of China (Grant No. 60872034, 60971029), in part by the New-Century Talent Program of the Education Department of China (Grant No. NCET070154), in part by the Funding of State Key Laboratory of Millimeter Waves (Grant No. K 00809), and in part by the Aviation Science foundation (Grant No. 20090180007).

REFERENCES

- [1] R. Shelby, D. Smith, and S. Schultz, "Experimental Verification of a Negative Index of Refraction," *Science* 292, 77, 2001.
- [2] G. Monti and L. Tarricone, "Dispersion Analysis of a Negative Group Velocity Medium with MATLAB," *Applied Computational Electromagnetic Society (ACES) Journal* 24, 5, 2009.
- [3] V. G. Veselago, "The Electrodynamics of Substances with Simultaneously Negative Values of ϵ and μ ," *Sov. Phys. Usp.* 10, 509, 1968.
- [4] R. W. Ziolkowski, "Design, Fabrication, and Testing of Double Negative Metamaterials," *IEEE Trans. Antennas Propag.* 51, 1516, 2003.
- [5] L. Ran, J. Huangfu, Y. Li, X. Zhang, K. Chen, and J. A. Kong, "Microwave Solid-State Left-Handed Material with a Broad Bandwidth and an Ultralow Loss," *Phys. Rev. B* 70, 073102,

- 2004.
- [6] H. Chen, L. Ran, J. Huangfu, X. Zhang, K. Chen, T. M. Grzegorzcyk, and J. A. Kong, "Negative Refraction of a Combined Double S-Shaped Metamaterial," *Appl. Phys. Lett.* 86, 151909, 2005.
- [7] N. T. Tung, V. T. T. Thuy, J. W. Park, J. Y. Rhee, and Y. P. Lee, "Left-Handed Transmission in a Simple Cut-Wire Pair Structure," *J. Appl. Phys.* **107**, 023530, 2010.
- [8] H. Chen, L. Ran, J. Huangfu, X. Zhang, K. Chen, T. M. Grzegorzcyk, and J. A. Kong, "Left-Handed Materials Composed of Only S-Shaped Resonators," *Phys. Rev. E* 70, 057605, 2004.
- [9] D. Wang, L. Ran, H. Chen, and M. Mu, "Experimental Validation of Negative Refraction of Metamaterial Composed of Single Side Paired S-Ring Resonators," *Appl. Phys. Lett.* 90, 254103, 2007.
- [10] E. Plum, J. Zhou, J. Dong, V. A. Fedotov, T. Koschny, C. M. Soukoulis, and N. I. Zheludev, "Metamaterial with Negative Index due to Chirality," *Phys. Rev. B* 79, 035407, 2009.
- [11] Z. Wang, D. Wang, T. Jiang, L. Peng, J. Huangfu, and L. Ran, "Very Simple Metallic Subwavelength Cell for Constructing Left-Handed Metamaterial," *Appl. Phys. Lett.* 94, 231905, 2009.
- [12] Y. -H. Liu, C. -R. Luo, and X. -P. Zhao, "H-Shaped Structure of Left-Handed Metamaterials with Simultaneous Negative Permittivity and Permeability," *Acta Phys. Sin.* 56, 5883, 2007.
- [13] J. B. Pendry, A. J. Holden, D. J. Robbins, and W. J. Stewart, "Magnetism from Conductors and Enhanced Nonlinear Phenomena," *IEEE Trans. Microwave Theory Tech.* 47, 2075, 1999.
- [14] Y. Yuan, C. Bingham, T. Tyler, S. Palit, T. H. Hand, W. J. Padilla, D. R. Smith, N. M. Jokerst, and S. A. Cummer, "Dual-Band Planar Electric Metamaterial in the Terahertz Regime," *Opt. Express* 16, 9746, 2008.
- [15] M. Tang, S. Xiao, T. Deng, and B. Wang, "Novel Folded Single Split Sing Resonator and its Application to Eliminate Scan Blindness in Infinite Phased Array," in *Proceedings of International Symposium on Signals, Systems and Electronics*, 2010, vol.1, p. 274.
- [16] W. J. Padilla, A. J. Taylor, C. Highstrete, Mark Lee, R. D. Averitt, "Dynamical Electric and Magnetic Metamaterial Response at Terahertz Frequencies," *Phys. Rev. Lett.* 96, 107401, 2006.
- [17] S. Linden, C. Enkrich, M. Wegener, J. Zhou, T. Koschny, C. M. Soukoulis, "Magnetic Response of Metamaterials at 100 Terahertz," *Science* 306, 1351, 2004.
- [18] J. Zhou, Th. Koschny, M. Kafesaki, E.N. Economou, J. B. Pendry, and C.M. Soukoulis, "Saturation of the Magnetic Response of Split-Ring Resonators at Optical Frequencies," *Phys. Rev. Lett.* 95, 223902, 2005.
- [19] M. V. Gorkunov, S. A. Gredeskul, I. V. Shadrivov, and Y. S. Kivshar, "Effect of Microscopic Disorder on Magnetic Properties of Metamaterials," *Phys. Rev. E* 73, 056605, 2006.
- [20] T. F. Gundogdu, I. Tsiapa, A. Kostopoulos, G. Konstantinidis, N. Katsarakis, R. S. Penciu, M. Kafesaki, E. N. Economou, Th. Koschny, and C. M. Soukoulis, "Experimental Demonstration of Negative Magnetic Permeability in Far-Infrared Frequency Regime," *Appl. Phys. Lett.* 89, 084103, 2006.
- [21] L. Jelinek, R. Marqués, and M. J. Freire, "Accurate Modeling of Split Ring Metamaterial Lenses for Magnetic Resonance Imaging Applications," *J. Appl. Phys.* 105, 024907, 2009.
- [22] A. A. Zharov, I. V. Shadrivov, and Y. S. Kivshar, "Nonlinear Properties of Left-Handed Metamaterials," *Phys. Rev. Lett.* 91, 037401, 2003.
- [23] T. J. Yen, W. J. Padilla, N. Fang, D. C. Vier, D. R. Smith, J. B. Pendry, D. N. Basov, and X. Zhang, "Terahertz Magnetic Response from Artificial Materials," *Science* 303, 1494, 2004.
- [24] H. T. Chen, W. J. Padilla, J. M. O. Zide, A. C. Gossard, A. J. Taylor, and R. D. Averitt, "Active Terahertz Metamaterial Devices," *Nature (London)* 444, 597, 2006.
- [25] M. Beruete, M. Sorolla, and I. Campillo, "Left-Handed Extraordinary Optical Transmission Through a Photonic Crystal of Subwavelength Hole Arrays," *Opt. Express* 14, 5445, 2006.
- [26] M. Beruete, I. Campillo, M. Navarro-Cia, F. Falcone, and M. S. Ayza, "Molding Left- or Right-Handed Metamaterials by Stacked Cutoff Metallic Hole Arrays," *IEEE Trans. Antennas*

- Propag.*, 55, 1514, 2007.
- [27] P. Ding, E. J. Liang, L. Zhang, Q. Zhou, and Y. X. Yuan, "Antisymmetric Resonant Mode and Negative Refraction in Double-Ring Resonators under Normal-to-Plane Incidence," *Phys. Rev. E* 79, 016604, 2009.
- [28] R. Marqués, F. Medina, and R. Rafii-El-Idrissi, "Role of Bianisotropy in Negative Permeability and Left-Handed Metamaterials," *Phys. Rev. B* 65, 144440, 2002.
- [29] D. R. Smith, J. Gollub, J. J. Mock, W. J. Padilla, and D. Schurig, "Calculation and Measurement of Bianisotropy in a Split Ring Resonator," *J. Appl. Phys.*, 100, 024507, 2006.
- [30] Z. -G. Dong, S. -Y. Lei, M. -X. Xu, H. Liu, T. Li, F. -M. Wang, and S. -N. Zhu, "Negative Index of Refraction in Metallic Metamaterial Comprising Split-Ring Resonators," *Phys. Rev. E* 77, 056609, 2008.
- [31] H. Chen, L. Ran, J. Huangfu, T. M. Grzegorzczak, and J. A. Kong, "Equivalent Circuit Model for Left-Handed Metamaterials," *J. Appl. Phys.*, 100, 024915, 2006.
- [32] S. I. Maslovski, S. A. Tretyakov, and P. A. Belov, "Wire Media with Negative Effective Permittivity: A Quasi-Static Model," *Microwave Opt. Tech. Lett.*, 35, 47, 2002.
- [33] D. R. Smith, D. C. Vier, Th. Koschny, and C. M. Soukoulis, "Electromagnetic Parameter Retrieval from Inhomogeneous Metamaterials," *Phys. Rev. E* 71, 036617, 2005.
- [34] Z. Szabó, G. -H. Park, R. Hedge, and E. -P. Li, "A Unique Extraction of Metamaterial Parameters Based on Kramers-Kronig Relationship," *IEEE Trans. Microwave Theory Tech.* 58, 2646, 2010.
- [35] T. Koschny, P. Markoš, D. R. Smith, and C. M. Soukoulis, "Resonant and Antiresonant Frequency Dependence of the Effective Parameters of Metamaterials," *Phys. Rev. E* 68, 065602, 2003.